Estuaries Vol. 28, No. 3, p. 338–352 June 2005

Flow Paths of Water and Sediment in a Tidal Marsh: Relations with Marsh Developmental Stage and Tidal Inundation Height

S. TEMMERMAN[1,2,*], T. J. BOUMA[2], G. GOVERS[1], and D. LAUWAET[1]

[1] *Katholieke Universiteit Leuven, Physical and Regional Geography Research Group, Redingenstraat 16, B-3000 Leuven, Belgium*

[2] *Netherlands Institute of Ecology (NIOO-KNAW), Centre for Estuarine and Marine Ecology, Korringaweg 7, 4401 NT Yerseke, The Netherlands*

ABSTRACT: This study provides new insights in the relative role of tidal creeks and the marsh edge in supplying water and sediments to and from tidal marshes for a wide range of tidal inundation cycles with different high water levels and for marsh zones of different developmental stage. Net import or export of water and its constituents (sediments, nutrients, pollutants) to or from tidal marshes has been traditionally estimated based on discharge measurements through a tidal creek. Complementary to this traditional calculation of water and sediment balances based on creek fluxes, we present novel methods to calculate water balances based on digital elevation modeling and sediment balances based on spatial modeling of surface sedimentation measurements. In contrast with spatial interpolation, the presented approach of spatial modeling accounts for the spatial scales at which sedimentation rates vary within tidal marshes. This study shows that for an old, high marsh platform, dissected by a well-developed creek network with adjoining levees and basins, flow paths are different for tidal inundation cycles with different high water levels: during shallow inundation cycles (high water level $<$ 0.2 m above the creek banks) almost all water is supplied via the creek system, while during higher inundation cycles (high water level $>$ 0.2 m) the percentage of water directly supplied via the marsh edge increases with increasing high water level. This flow pattern is in accordance with the observed decrease in sedimentation rates with increasing distance from creeks and from the marsh edge. On a young, low marsh, characterized by a gently seaward sloping topography, material exchange does not take place predominantly via creeks but the marsh is progressively flooded starting from the marsh edge. As a consequence, the spatial sedimentation pattern is most related to elevation differences and distance from the marsh edge. Our results imply that the traditional measurement of tidal creek fluxes may lead in many cases to incorrect estimations of net sediment or nutrient budgets.

Introduction

The widely recognized ecosystem value of tidal marshes (e.g., as feeding and breeding areas for fish, shellfish, crustaceans, and birds) is often conflicting with the human use of coasts and estuaries (e.g., for shipping, agricultural, industrial, or urban development), which has resulted in protective regulations for tidal marshes (e.g., Ramsar Convention, http://www.ramsar.org; European Community Birds and Habitats Directives, http://www.ecnc.nl). In order to support protective measures, there is a need for fundamental understanding of the highly dynamic functioning of tidal marsh ecosystems. Tidal marshes are regularly flooded, during which suspended and dissolved constituents, such as sediments, nutrients, and pollutants, are transported to and partly deposited within the marsh system. These tidal fluxes of water, sediments, and nutrients, which occur on the time scale of a single tidal cycle, are the key to understanding the long-term (10–100 yr) geomorphological and ecological evolution of tidal marshes. Net sediment deposition and the resulting vertical rise of tidal marshes ultimately determine the ability of the tidal marsh vegetation to survive sea-level rise.

Tidal marshes are typically dissected by tidal creeks, which start from the seaward marsh edge and branch, narrow and shallow inland. The measurement of flood and ebb discharges through tidal creeks has been traditionally used to quantify net material fluxes of sediments (e.g., Settlemyre and Gardner 1977; Reed et al. 1985; Stevenson et al. 1985; Leonard et al. 1995b; Suk et al. 1999) or nutrients (e.g., Webb et al. 1983; Dame et al. 1991) between tidal marshes and the adjacent sea or estuary. This method has been used to identify the influence of external factors, such as tidal amplitude or wind-wave activity, on the import or export of material to or from tidal marshes (e.g., Stevenson et al. 1988; Leonard et al. 1995b).

Although widely used, the measurement of tidal creek fluxes does not account for fluxes that may

* Corresponding author; current address: Netherlands Institute of Ecology (NIOO-KNAW), Centre for Estuarine and Marine Ecology, Korringaweg 7, 4401 NT Yerseke, The Netherlands; tele: +31 113 577452; fax: +31 113 573616; e-mail: s.temmerman@nioo.knaw.nl

occur via the seaward marsh edge instead of the creek system. As a consequence, creek flux measurements alone may lead to incorrect estimations of material import and export (French and Stoddart 1992; French et al. 1995). Flux measurements in tidal creeks only aim at identifying net fluxes between tidal marshes and the adjacent coastal or estuarine system, but do not reveal transport pathways within marshes. These internal flow paths are crucial to identify where sinks or sources of material are located within the marsh system and to identify internal marsh mechanisms underlying net import or export of material.

These shortcomings of flux measurements in tidal creeks are partially countered when using a spatial network of measuring sites. In the case of sediment fluxes and on the time scale of single tidal cycles, spatial networks of sediment traps have been used to sample the sediment that settled out on the marsh surface (French et al. 1995; Leonard 1997; Davidson-Arnott et al. 2002). Spatial variations in sediment deposition within marshes are typically high (e.g., Stoddart et al. 1989; French and Spencer 1993; Temmerman et al. 2003). As a consequence, difficulties arise if overall sediment fluxes to a certain marsh area are aimed to be calculated; these calculations are traditionally based on averaging or spatial interpolation of point measurements of sediment deposition on sediment traps (French et al. 1995). Averaging or spatial interpolation does not account for the spatial scales at which sedimentation rates typically vary, so that the measuring network needs to be dense enough to cover the spatial variations in sedimentation rates.

As sketched above, earlier studies focused either on tidal creek fluxes or on marsh surface processes, but very few studies paid attention to the interaction between both. French and Stoddart (1992) demonstrated that about 40% of the total water flux occurred via the marsh edge instead of the creek system, for 4 tidal cycles on a North Norfolk (U.K.) salt marsh. French et al. (1995) showed that large discrepancies exist between net sediment fluxes calculated from creek flux measurements and from a spatial network of surface sedimentation measuring sites, for one tidal cycle in the same study area. These studies were limited to only a few particular tidal cycles and 1 particular salt marsh topography. Up to now, it is largely unclear how the percentage of material exchange via creeks versus the marsh edge varies between a large number of tidal cycles, e.g., as a consequence of differences in high water level or wind-driven flow paths, and between marshes with a different topography.

We present an analysis of water and sediment balances for a large number of tidal cycles and marsh zones with different topographies, based on both creek flux measurements and spatially distributed marsh surface measurements within the same study area. The presented analyses provide novel insights into the relative role of tidal creeks in supplying water and sediments to and from tidal marshes for a wide range of tidal inundation cycles with different high water levels and for marsh zones of different developmental stage. Complementary to the traditional calculation of water and sediment balances, based on creek flux measurements, novel methods are presented to calculate water balances based on high-resolution digital elevation modeling and sediment balances based on spatial modeling of surface sedimentation measurements. In contrast with spatial interpolation, the presented approach of spatial modeling accounts for the spatial scales at which sedimentation rates vary.

Study Area

The study was carried out at Paulina marsh, a salt marsh situated in the Scheldt estuary, southwest Netherlands (Fig. 1). The local tidal regime is semidiurnal, with a mean tidal range of 3.9 m (Claessens and Meyvis 1994). The time-averaged suspended sediment concentration in the nearby estuarine stream channel is about 30 mg l^{-1} near the water surface (Van Damme et al. 2001).

Different stages in the geomorphological development and vegetational succession of salt marshes are present in the study area. A clear distinction can be made between two zones within the same marsh: an old, high salt marsh zone (already present on topographic maps of 1856) and a young, low salt marsh zone (formed around 1980; Fig. 1). The old, high marsh is characterized by a relatively flat topography and well-developed tidal creek system and levee-basin topography between the creeks. It has northwestern European salt marsh species, such as *Elymus pycnanthus* on the highest levees and *Halimione portulacoides, Aster tripolium,* and *Puccinellia maritima* in the lower basins. The young, low marsh gradually slopes down to the seaward marsh edge, with fewer tidal creeks than the high marsh and no levee-basin topography. The low marsh is dominated by a pioneer vegetation of *Spartina anglica.* A bare tidal flat is present in front of the seaward marsh edge.

The field measurements were carried out within one small tidal creek catchment (56,000 m^2), which contains parts of the high and low marsh zone (Fig. 1). A tidal creek catchment is defined here as the marsh area that is flooded and drained by one tidal creek beginning at the marsh edge and branching into a dendritic creek system. No real interfluves are present between adjacent creek

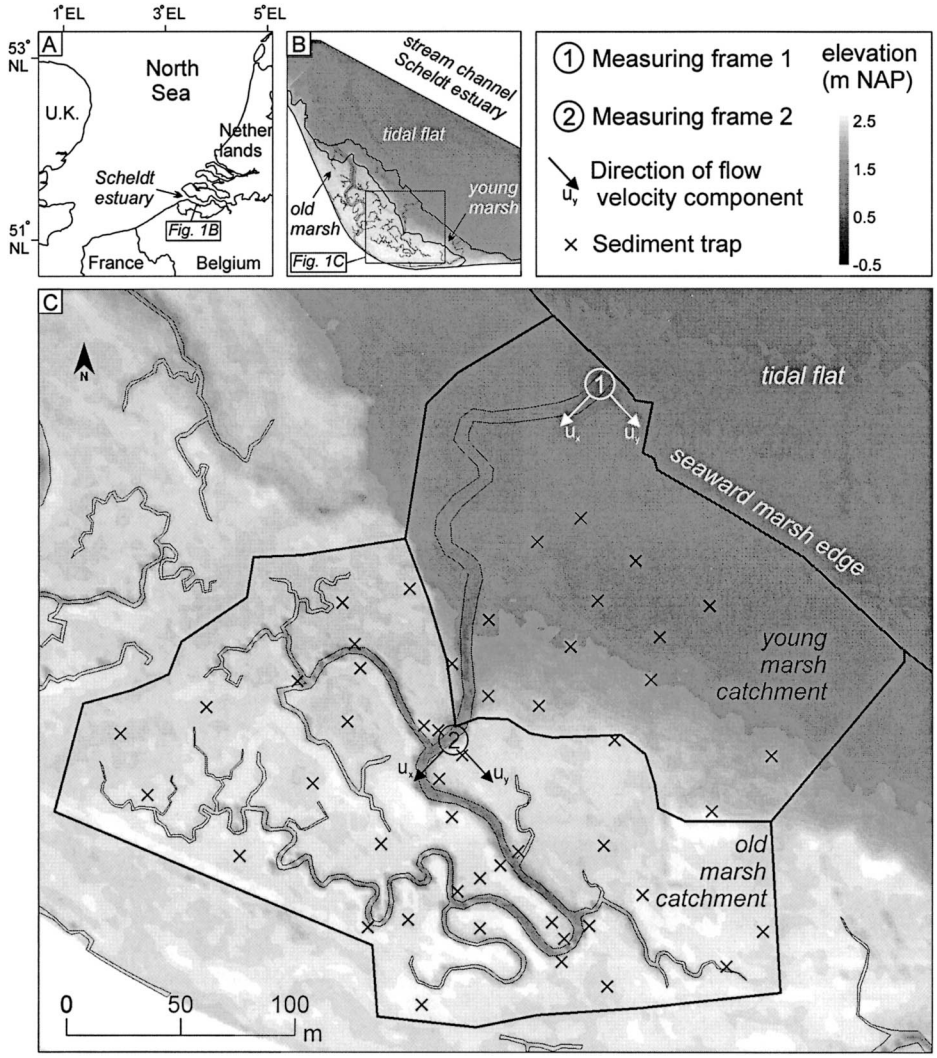

Fig. 1. Map of the study area, Paulina marsh: (A) location within Western Europe; (B) digital elevation model (DEM), with indication of the young and old marsh; (C) detail of the DEM showing the studied tidal creek catchment, the location of measuring frames 1 and 2, the direction of flow velocity components u_x and u_y measured at frames 1 and 2, and the location of sediment traps.

catchments, so that additional exchanges of water and sediment between adjacent catchments can not be a priori excluded.

Methods

Tidal Creek Measurements

A large interdisciplinary field measuring campaign was carried out in the study area from June to October 2002 (see Bouma et al. [In press] for a general overview). Within the studied creek system, measuring frames were installed at two locations (Fig. 1): frame 1 was installed at the mouth of the creek at the seaward marsh edge, with the intention to measure material fluxes to and from the entire creek catchment (both low and high marsh); frame 2 was placed deeper into the creek at the edge between the low and high marsh, in order to measure fluxes to and from the high marsh part of the creek catchment only.

Both measuring frames were equipped with a pressure sensor to measure vertical water level movements due to the tide (in meters relative to Dutch ordnance level, NAP), a bidirectional electromagnetic flow meter (EMF) to measure flow velocities (in m s^{-1}) at 7 cm above the bottom, and an optical backscatter sensor (OBS) to measure turbidity (in FTU = Formazine Turbidity Units) at 15 cm above the bottom. Data were collected with a frequency of 4 Hz during 6 h around each high water (i.e., the time that the frames were submerged by the tide) from June 11 to October 2, 2002 (i.e., 222 tides). The 4-Hz data files were pro-

cessed to time series of 1-min averages and 15-min averages.

In order to calibrate the OBS data (in FTU) to suspended sediment concentrations (SSC; in g l^{-1}), an automatic water sampling station was installed next to frame 2, equipped with an ISCO 6700 water sampler that pumped 1 l water samples near the OBS sensor. For every semidiurnal tidal cycle, one sample was collected at flood tide when the water level exceeded 0.5 m above the creek bottom. During 4 semidiurnal cycles (August 11 and 12, 2002 and September 10 and 11, 2002), water samples were taken with a time interval of 30 min during the whole inundation cycle, until the sampling location was no longer submerged. During the same 4 inundation cycles, additional water samples were collected at different heights in the water column (0.20, 0.70, and 1.35 m above the creek bottom). All collected water samples were filtered with preweighed filter papers (pore diameter = 0.45 μm), which were subsequently washed with deionized water to remove salts and then oven-dried for 24 h at 50°C and reweighed.

Measuring the Spatial Sedimentation Pattern

The sediment that was deposited on the marsh surface was sampled at 50 sites randomly distributed within the catchment of the studied creek system (Fig. 1). Two sampling methods were used, depending on the time scale of the measurements. During two biweekly spring-neap tidal cycles (August 5–20, 2002 and September 2–16, 2002), the deposited sediment was sampled using plastic circular sediment traps (diameter = 0.233 m). The traps were constructed with a floatable cover to protect the deposited sediment from splash by raindrops during low tide (cf., Temmerman et al. 2003). During the measuring period, no significant wind-wave activity was measured in the study area (Bouma et al. In press). The traps were attached to the marsh surface at neap tide and collected again 15 d later at the following neap tide. In the laboratory, the deposited sediment was washed from the traps, rinsed with deionized water to remove salts, and sieved at 707 μm to remove macroscopic plant or shell material. The remaining sediment was oven-dried at 50°C and weighed to determine the sedimentation rate (in g m^{-2} per spring-neap cycle).

In addition to the plastic sediment traps, filter paper traps (diameter = 0.15 m; pore diameter = 0.45 μm; e.g., Reed 1989; French et al. 1995; Leonard 1997) were used to sample the sediment that was deposited during 4 semidiurnal inundation cycles (August 11 and 12, 2002 and September 10 and 11, 2002). The filter papers were attached to aluminium plates and fixed to the marsh surface just before and collected after tidal inundation. The filter papers were washed to remove salts, oven-dried for 24 h at 50°C, and reweighed to determine the sedimentation rate (in g m^{-2} per semidiurnal tide).

The spring-neap data were not normalized to sedimentation rates in g m^{-2} per semidiurnal tidal cycle because during the spring-neap cycles there were semidiurnal tidal cycles that flooded the study area only partially (e.g., only the low marsh sites and not the high marsh sites) and different kinds of sediment traps were used for the spring-neap and semidiurnal periods. All analyses explained below were conducted separately for the spring-neap and semidiurnal data sets.

Calculating Water Balances

Based on Tidal Creek Hydrodynamics

The total water volumes that were transported through the creek system during flood (V_F in m^3) and ebb (V_E in m^3) were calculated as:

$$V_F = \int_F u \times A(h)\, dt \quad \text{and}$$

$$V_E = \int_E u \times A(h)\, dt \qquad (1)$$

where u = flow velocity (in m s^{-1}; 15-min averages of the EMF measurements), and A(h) = the wet cross section of the creek (in m^2). The creek cross section was surveyed at each frame in order to calculate A(h) for any water level h at time t. For water levels exceeding bankfull water level, A(h) was calculated as:

$$A(h) = A(h)_{bf} + w \times (h - h_{bf}) \qquad (2)$$

where $A(h)_{bf}$ = the wet cross section at bankfull water level (= 4.5 m^2 at frame 2), w = the creek width (= 3 m at frame 2), and h_{bf} = bankfull water level. At the creek mouth at frame 1, no clearly incised creek is present but the general marsh surface topography is rather flat (Fig. 1), so A(h) was calculated here as:

$$A(h) = w \times h \qquad (3)$$

where w = 7 m = the width of the creek where it begins to incise at a few tens of meters behind the creek mouth at frame 1 (see Fig. 1).

As indicated in earlier studies, the error on calculations of tidal creek fluxes depends on temporal and spatial sampling of flow velocities, which may vary both laterally and vertically within the creek cross section (e.g., Boon 1978; Ward 1981; Reed 1987; Leonard et al. 1995b). We examined the influence of temporal sampling by solving Eq. 1 using 1-min and 15-min average flow velocities

calculated from the 4-Hz raw data for 4 tidal cycles. The maximum difference in calculated V_F and V_E values based on both time intervals was 3%. For all other tidal cycles, the 15-min averages were used.

Since we used only one sampling location, we have no data on spatial variations in velocities within the creek cross section. Vertical variations in sediment concentration, which were measured at 0.20, 0.70, and 1.35 m above the creek bottom during flood tide for 4 tidal cycles, were rather small (< 9% variation), indicating that well-mixed flow conditions prevailed. This supports the use of only one sampling location. Other tidal flux studies in large creeks (15–50 m wide) indicated that errors due to spatial variations and the use of only one sampling location are in the order of 5–15% at most (Ward 1981; Stevenson et al. 1985; Leonard et al. 1995b; Suk et al. 1999). In this study, where a much smaller creek of 3–7 m wide was monitored, we may assume then that the error due to both temporal and spatial sampling will be in the order of 10%.

Based on Digital Elevation Modeling

The total water volume V_{HW} stored at high tide above the marsh surface was calculated using a digital elevation model (DEM) with a resolution of 1 × 1 m (Fig. 1). The DEM was calculated in Surfer (Golden Software, Inc., Colorado) by spatial interpolation (triangulation with linear interpolation) of an extensive data set of elevation points (in m NAP) with a resolution of 3 × 3 m. This data set was collected in 2001 by the Dutch Topographic Survey (Van Heerd and Van't Zand 1999) by LiDAR (light-induced direction and ranging), which is a relatively recent technique through which the elevation of the earth surface is surveyed by laser scanning from an airplane (e.g., Measures 1991; French 2003). In order to calculate the water volumes V_{HW}, we assumed that the water surface was horizontal at high tide, which is a realistic assumption for such a small study area. V_{HW} was then calculated for semidiurnal tidal cycles with different high water levels $h(t_{HW})$ (in m NAP) as:

$$V_{HW} = \sum_i a_i \times h_i \quad \text{where}$$

$$h_i = \begin{cases} h(t_{HW}) - z_i & \text{if } h(t_{HW}) - z_i > 0 \\ 0 & \text{if } h(t_{HW}) - z_i \le 0 \end{cases} \quad (4)$$

where a_i = the surface area of raster cell i of the DEM (= 1 m^2), h_i = the water depth at raster cell i, and z_i = the marsh surface elevation at raster cell i. In order to compare V_{HW} with V_F and V_E, calculated for frame 1 (representative for both the young and old marsh) and for frame 2 (representative for the old marsh only), V_{HW} values were calculated separately for the young and old marsh part of the studied creek catchment (Fig. 1).

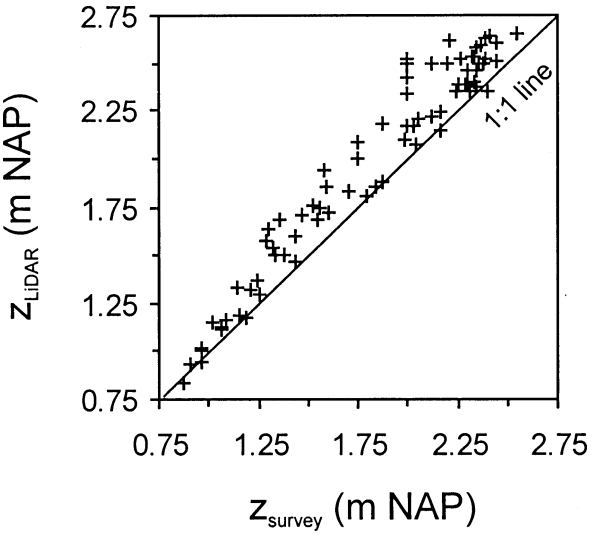

Fig. 2. Comparison between elevations determined from field surveys (z_{survey}) and from LiDAR measurements (z_{LiDAR}) for 76 control points.

Based on aerial photographs, the surface area of the creek catchment was delineated by the apparent interfluves between the studied catchment and neighboring creek catchments. No real topographic interfluves are present between creek catchments in tidal marshes. In order to estimate the error on V_{HW} due to this uncertainty in the catchment area, V_{HW} values were also calculated for catchment areas that were 10 m wider and 10 m narrower than the originally defined catchment area. This buffer of 10 m is realistic, since the maximum distance between adjacent creeks is about 40 m in the study area.

A second source of error is related to the vertical inaccuracy of the LiDAR elevation data. In order to estimate this vertical inaccuracy, the elevation of the marsh surface was surveyed at 76 locations within the study area relative to local benchmarks (in m NAP) with an electronic total station (SET5F, Sokkia, Co., Ltd., Kanagawa, Japan). A good correlation was found between the elevation of these field survey points (z_{survey}) and the DEM generated from the LiDAR data (z_{LiDAR}) ($R^2 = 0.95$) and the mean elevation difference $z_{LiDAR} - z_{survey}$ was 0.15 m with a standard deviation of 0.13 m (Fig. 2). Vertical errors on total station measurements are in the order of millimeters only, so that almost all of this difference can be attributed to the LiDAR measurements: the mean difference of 0.15 m is caused by laser reflection on the marsh vegetation cover instead of on the earth surface; the standard deviation of 0.13 m can be interpreted as vertical

inaccuracy related to the LiDAR technology (see e.g., Baltsavias 1999). Before calculation of V_{HW}, the DEM was lowered by 0.15 m to correct for the marsh vegetation.

To estimate the combined error on V_{HW} due to the error on the catchment area and LiDAR elevations, a smallest possible V_{HW} value was calculated using the narrower catchment area and DEM lowered by [0.15 − 0.13] m, and a largest possible V_{HW} value was calculated using the wider catchment area and DEM lowered by [0.15 + 0.13] m.

Calculating Sediment Balances

Based on Sediment Transport Through Tidal Creeks

Similar to the calculation of V_F and V_E, as explained above, the total suspended sediment mass transported through the creek system during flood (TSS_F) and ebb (TSS_E) was calculated, separately for frame 1 and 2, as:

$$TSS_F = \int_F u \times A(h) \times C \, dt \quad \text{and}$$

$$TSS_E = \int_E u \times A(h) \times C \, dt \qquad (5)$$

where C is SSC (in g l^{-1}) at time t. The net import or export of suspended sediment over one semidiurnal tidal cycle was then calculated as:

$$TSS_{net} = TSS_F + TSS_E \qquad (6)$$

Similar to the error estimation on the water flux calculations above, we may assume that the error on the sediment flux calculations will be in the order of 10%.

Based on Spatial Modeling of Sedimentation

The total suspended sediment mass that was deposited on the marsh surface (TSS_{dep}) was calculated from the 50 sedimentation rate measurements using three methods: multiplying the mean of the 50 sedimentation rate measurements (g m^{-2} per semi-diurnal cycle or spring-neap cycle) with the surface area of the creek catchment (m^2); spatial interpolation (point Kriging) of the point measurements over a raster grid of 1 × 1 m and summing the interpolated sedimentation rates over all raster cells within the catchment area (the first two methods are in accordance with French et al. [1995]); and spatial modeling of the sedimentation pattern (see below). For all three methods, the surface area occupied by tidal marsh creeks was excluded, so that the calculated TSS_{dep} values only apply to the vegetated marsh platform. The calculations were performed separately for the high and low marsh part of the creek catchment. The error on TSS_{dep}, due to the error on the surface area of the creek catchment, was also estimated using the wider and narrower catchments with a buffer of 10 m.

For the third method, we used a topography-based regression model describing the spatial variations in sedimentation rates, which was originally presented in Temmerman et al. (2003):

$$SR = k \times e^{lH} \times e^{mD_c} \times e^{nD_e} \qquad (7)$$

where SR = sedimentation rate (g m^{-2} per time interval, here per spring-neap cycle or semidiurnal cycle), H = elevation of the marsh surface (m NAP), D_c = distance from the nearest tidal creek (m), D_e = distance from the marsh edge, measured along the nearest creek (m). k, l, m, and n are regression parameters.

This model is a simple representation of the mechanisms thought to control spatial variations in sedimentation rates. Less sediment is deposited on marsh parts with a higher elevation, H, as a consequence of a decrease in inundation frequency, height, and duration with increasing marsh elevation. The model parameter l is then a measure for how fast sedimentation rates decrease with increasing marsh surface elevation, H. The model assumes that sedimentation rates decrease with increasing distance from creeks, D_c, and from the marsh edge, D_e, as a consequence of progressive settling of suspended sediments on their transport pathway from the marsh edge and from the creeks to the inner marsh. The model parameters m and n are then a measure for how fast sedimentation rates decrease with increasing distance from creeks, D_c, and increasing distance from the marsh edge, D_e, respectively. The model parameter k is a measure for the overall, total amount of sediment that is deposited in the study area; the larger k is, the more sediment is deposited.

This model was used to analyze the spatial sedimentation pattern that was observed with the network of 50 sedimentation rate measuring sites. Values were determined for the model variables H, D_c, D_e, and SR for each of the 50 measuring sites, based on field data. The elevation, H, was surveyed in the field using an electronic total station (SET5F, Sokkia, Co., Ltd., Kanagawa, Japan). The variables D_c and D_e were calculated in a geographic information system (GIS) based on the planform of the tidal creek system that was digitized from a geo-referenced aerial photograph, and using the nearest distance algorithms DISTANCE, COST, and ALLOCATE in Idrisi (Eastman 1994). Time-averaged sedimentation rates, SR, were calculated for the 2 spring-neap cycles and for the 4 semidiurnal cycles that were sampled in order to concentrate on the spatial variation between the 50 measuring sites. This procedure of time-averaging is ac-

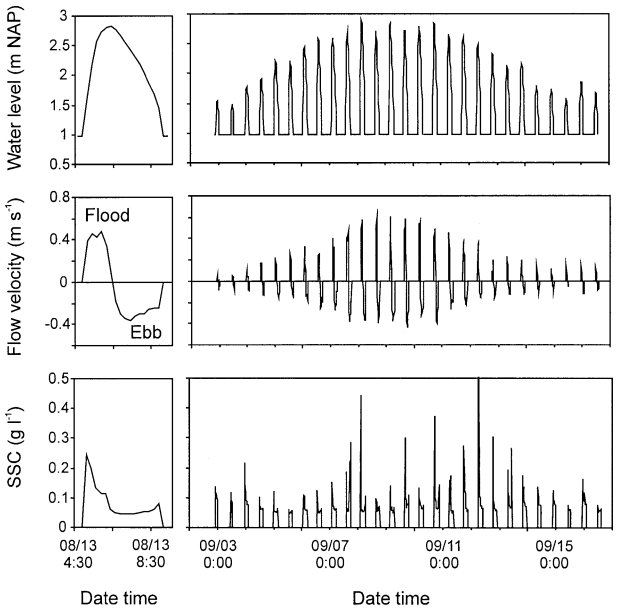

Fig. 3. Example of time series of water level, flow velocity, and suspended sediment concentration (SSC) recorded by measuring frame 2 during a semidiurnal tidal cycle (left) and during a biweekly spring-neap cycle (right).

ceptable, since no significant difference was found between the 2 spring-neap data sets (*t*-test: $p = 0.06$) and between the 4 semidiurnal data sets (ANOVA: $p = 0.77$). This is because during the measuring periods the same range of tidal inundation heights and durations occurred, which are the most important factors controlling temporal variations in marsh sedimentation in the Scheldt estuary (Temmerman et al. 2003).

The model parameters k, l, m, and n were determined separately for the time-averaged spring-neap data set and time-averaged semidiurnal data set. This was done using the following procedure. Both data sets, containing 50 sedimentation measuring sites, were sorted from the lowest up to the highest measured sedimentation rate. Measuring sites with an even ranking number were used for calibration of k, l, m, and n, by stepwise multiple regression (using Eq. 7) between the observed time-averaged sedimentation rates, SR, and related H, D_c, and D_e values. Measuring sites with an uneven ranking number were used for model validation, by calculation of the sedimentation rates at these sites using the k, l, m, and n values resulting from the calibration, and by comparing calculated with observed sedimentation rates. Once validated, the model was spatially implemented in a 1×1 m raster GIS to compute TSS_{dep}, using spatial maps of H (i.e., the DEM), D_c, and D_e (both calculated in GIS as explained above) as input for the model.

Results

Temporal Patterns of Tidal Creek Hydrodynamics and SSC

The time series of water level and flow velocities that were recorded at frames 1 and 2 are very typical for tidal marsh creeks. At the time scale of individual semidiurnal tidal cycles, a clear tidal asymmetry is observed; both the rate of water level change and the maximum flow velocities are higher during flood than during ebb (Fig. 3). At the time scale of a spring-neap tidal cycle, maximum flow velocities are highest during spring tides and lowest during neap tides. Typical flow velocity pulses were observed in the creek; during over-marsh tides (i.e., tides that overtop the creek banks and flood the high marsh surface), flow velocity pulses were observed at frame 2 at the moment of flooding and draining of the surrounding high marsh platform, while these velocity pulses were absent during under-marsh tides (i.e., tides that do not overtop the creek banks; Fig. 4). At frame 1 at the marsh edge, these velocity pulses were not observed.

The OBS data (in FTU) from frames 1 and 2 could be calibrated to SSC data (in g l^{-1}), based on a good correlation between the OBS and SSC

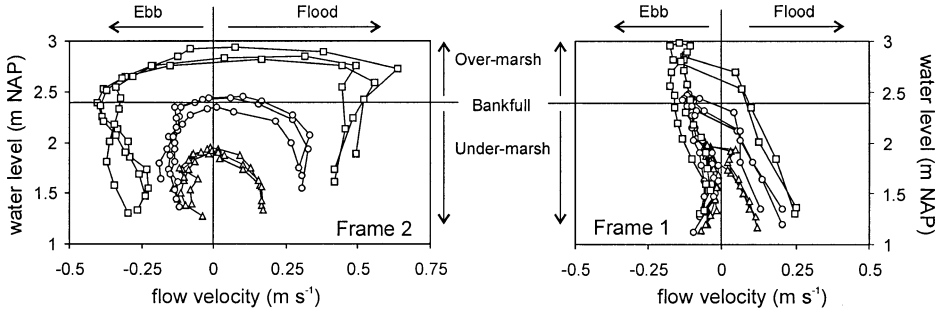

Fig. 4. Water level flow velocity curves for frame 2 and frame 1, for a number of randomly chosen under-marsh tides (triangles), bankfull tides (circles), and over-marsh tides (squares). Each curve represents one tide. Bankfull level is defined here as the level of the old, high marsh platform.

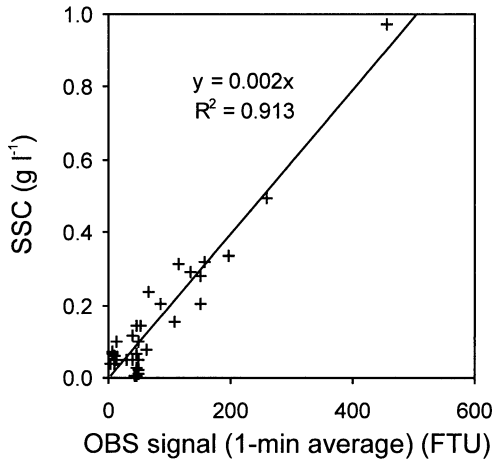

Fig. 5. Relationship between suspended sediment concentration (SSC) and optical back scatter (OBS) signal measured at 0.15 m above the bottom at frames 1 and 2.

values that were measured at the same time in the field (Fig. 5). At the time scale of individual semidiurnal tidal cycles, clear peaks in SSC were observed at the beginning and (in some cases) at the end of an inundation cycle (Fig. 3). The SSC between these two peaks did not vary significantly, but remained at a rather constant value of about 0.03–0.05 g l^{-1}. At the time scale of a spring-neap tidal cycle, the highest SSC peaks generally occurred during spring tides (Fig. 3). But we found no significant relationship between maximum SSC and high water level for different tidal cycles ($R^2 < 0.01$, $p = 0.75$).

Spatial Patterns of Sediment Deposition

The spatial sedimentation pattern, as observed in the study area, is primarily determined by much higher sedimentation rates on the low than on the high marsh, both for the 2 spring-neap cycles and for the 4 semidiurnal tidal cycles that were sampled (Fig. 6). On the high marsh, sedimentation rates were higher on creek banks (defined as regions within 3 m from the tidal creeks) than in the inner basins (> 3 m from the creeks). Statistical *t*-tests on the log-transformed sediment trap data showed that these spatial differences between the high and low marsh and between the creek banks and basins were significant for most measuring periods (Table 1).

The observed spatial sedimentation pattern was initially analyzed separately for the low and high marsh sites using the topography-based model in Eq. 7. Stepwise multiple regression showed that on the high marsh all three model variables H (elevation), D_c (distance from the nearest creek), and D_e (distance form the marsh edge measured along the nearest creek) have a similar share in explaining the spatial variations in sedimentation rates (Table 2). On the young marsh the spatial sedimentation pattern is most related to H and D_e.

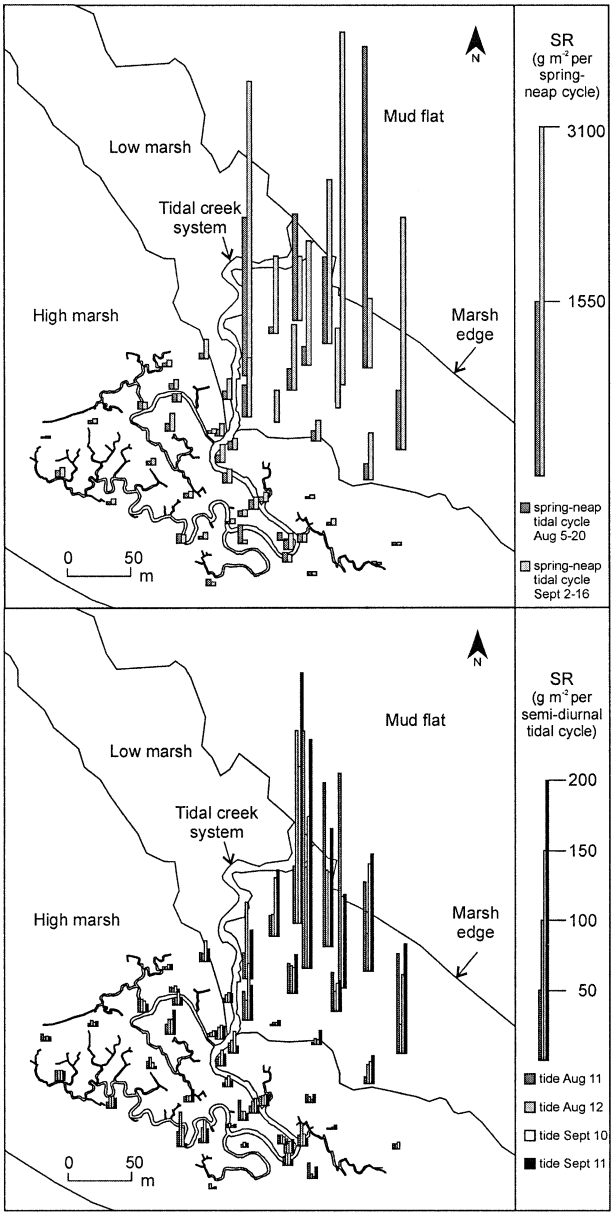

Fig. 6. The spatial sedimentation pattern measured over two spring-neap cycles (sedimentation rates, SR, in g m^{-2} per spring-neap cycle) and four semidiurnal tidal cycles (sedimentation rates, SR, in g m^{-2} per semidiurnal tidal cycle). For some locations and measuring periods, sediment traps were lost and consequently no data are presented.

The model was then calibrated and validated against the complete data set, including both the old and young marsh sites. Initial calibration resulted in good agreement between observed and predicted sedimentation rates, both for the spring-neap and semidiurnal data sets ($R^2 = 0.94$, $p <$

TABLE 1. p values resulting from *t*-tests comparing sedimentation rates on the high marsh versus sedimentation rates on the low marsh and sedimentation rates on creek banks (< 3 m from creeks) versus sedimentation rates in basins (> 3 m from creeks).

	Spring-neap Cycles		Semindiurnal Cycles			
	August 5–20	September 2–16	August 11	August 12	September 10	September 11
High versus low marsh	<0.01	<0.01	<0.01	<0.01	<0.01	<0.01
Creek banks versus basins	<0.01	<0.01	0.16	<0.01	<0.01	0.26

0.0001 in both cases; see Table 3 run 1 calibration). For the validation data sets the correspondence between observed and predicted sedimentation rates was rather poor ($R^2 = 0.51$, $p = 0.0003$ and $R^2 < 0.01$, $p = 0.9023$, respectively; see Table 3 run 1 validation). The calibration of run 1 resulted, illogically, in a positive m value for the spring-neap data set and in positive m and n values for the semidiurnal data set (Table 3). These positive values indicated that sedimentation rates would increase with increasing distance D_c from the creeks and increasing distance D_e from the marsh edge. This is in contradiction with Fig. 6 and the *t*-tests summarized in Table 1, which indicated that sedimentation rates on the high marsh were significantly higher on creek bank sites, just next to tidal creeks, than on basin sites, farther away from creeks. The positive m and n values were obtained because the highest sedimentation rates were observed on low marsh sites, although these sites were located the greatest distance from tidal creeks (see Fig. 6). These highest sedimentation rates on the low marsh were due to the low surface elevation and not to the large distance from creeks. On the low marsh no dense tidal creek system has developed as on the high marsh. As indicated by the stepwise multiple regression (Table 2), the influence of surface elevation, H, and distance from the marsh edge, D_e, on the sedimentation rates on the low marsh is more important than the influence of distance from creeks, D_c.

In order to account for this effect of the absence of tidal creeks on the low marsh, a critical threshold distance $D_{c,cr}$ was introduced; once the distance to the nearest creek, D_c, is larger than $D_{c,cr}$, we may say that the influence of D_c and D_e is negligible relative to the influence of the marsh surface elevation, H. This was modeled by setting D_c and D_e to zero for measuring sites for which $D_c > D_{c,cr}$. $D_{c,cr}$ was set here to 40 m, because this is about the maximum distance between tidal creeks on the high marsh platform with a well-developed tidal creek system. Calibration of this modified model resulted in negative m and n values, both for the spring-neap and semidiurnal data sets (see Table 3 run 2). The calibration and validation resulted in an acceptable match between predicted and observed sedimentation rates (Fig. 7).

Comparison of Water and Sediment Balances

The water volumes V_F and V_E (Eq. 1) discharged through the creek system during flood and ebb, respectively, were compared with the total water volume V_{HW} (Eq. 4) stored at high tide above the marsh surface for tidal cycles with a wide range of high water levels (Fig. 8). For frame 2 (representative for the high marsh), V_F and V_E were very comparable to V_{HW} for under-marsh tides and for over-marsh tides with a high water level lower than ca. 0.2 m above the high marsh platform. This means that for these tides the tidal creek system accounted for ca. 100% of the total water volume transported to and from the high marsh. For tidal cycles with a high water level higher than 0.2 m above the high marsh, the percentage of water that was supplied via the creek system progressively decreased with increasing high water level. As a consequence, an increasing percentage of water was supplied via other flow paths, such as directly across the marsh edge. V_F and V_E values were comparable for all tidal cycles, indicating that the water followed the same transport pathways during flood and ebb to and from the high marsh.

For frame 1 (representative for the low and high

TABLE 2. R^2 values resulting from stepwise multiple regression analysis using as the independent variable in Eq. 7: (1) only H (m, n = 0), (2) only D_c (1, n = 0), (3) only D_e (1, m = 0), (4) H and D_c (n = 0), (5) H and D_e (m = 0), (6) D_c and D_e (1 = 0), and (7) H, D_c, and D_e.

Marsh	Data Set	(1) H	(2) D_c	(3) D_e	(4) H, D_c	(5) H, D_e	(6) D_c, D_e	(7) H, D_c, D_e
Old	Spring-neap	0.42	0.43	0.47	0.56	0.61	0.58	0.67
	Semidiurnal	0.27	0.28	0.24	0.36	0.28	0.30	0.38
Young	Spring-neap	0.43	0.09	0.63	0.44	0.63	0.67	0.78
	Semidiurnal	0.78	0.28	0.63	0.83	0.80	0.64	0.86

TABLE 3. Model parameters (k, l, m, n), R^2, and p values resulting from calibration and validation of the topography-based model (Eq. 7). Run 1: H, D_c, and D_e determined from GIS analyses; Run 2: idem, but D_c and D_e are set to zero for measuring sites for which $D_c > 40$ m (see text for more details).

						Calibration		Validation	
Run	Data Set	k	l	m	n	R^2	p	R^2	p
1	Spring-neap	301.4	−0.4935	0.0344	−0.0023	0.94	<0.0001	0.51	0.0003
	Semidiurnal	1609.5	−3.7115	0.0026	0.0086	0.94	<0.0001	<0.01	0.9023
2	Spring-neap	1067.0	−0.2174	−0.0102	−0.0080	0.69	<0.0001	0.63	<0.0001
	Semidiurnal	281.1	−1.2659	−0.0417	−0.0022	0.87	<0.0001	0.74	<0.0001

marsh), both V_F and V_E were much lower than V_{HW} (Fig. 8). This indicates that the supply of water to and from the low marsh did not take place at frame 1 only. Since no clear incised creeks are present along the marsh edge (Fig. 1), it is more likely that the exchange of water took place along the entire length of the marsh edge. For all tidal cycles, V_F was considerably lower than V_E. This is because during a large part of the ebb phase of the tidal cycle, flow directions were not perpendicular to but rather parallel to the marsh edge (Fig. 9). Only at the beginning and end of a tidal inundation cycle were flow directions more or less perpendicular to the marsh edge. The large V_E values reflected along-shore water movement (parallel to the marsh edge) instead of offshore water movement (export perpendicular to the marsh edge).

The calculated total sediment masses that were deposited on the marsh surface (TSS_{dep}) were slightly different for the three calculation methods that were used (Fig. 10). For frame 2 TSS_{dep} values calculated by spatial modeling were systematically lower than TSS_{dep} values calculated by averaging and spatial interpolation (Kriging). This is because on the high marsh many of the measuring sites (15 of 34, i.e., 44%) were located on a creek bank (< 3 m from creeks), where high sedimentation rates were measured, while the total area of creek banks was calculated as only 24% of the total high marsh platform area. As a consequence, averaging and Kriging of the 34 high marsh measurements resulted in higher TSS_{dep} values than spatial modeling, since the latter accounts for the rapid (exponential) decrease of sedimentation rates with increasing distance from the creeks.

For frame 2, a net import of suspended sediments via the creek system ($TSS_{net} > 0$) was calculated for all monitoring periods (Fig. 10). The TSS_{net} values at frame 2 were for all measuring periods of the same order of magnitude as TSS_{dep} values calculated for the high marsh platform. This suggests that the creek system served as the major transport pathway of sediments to the high marsh platform. Although TSS_{net} values were not significantly different from TSS_{dep} values, TSS_{net} seemed to be slightly higher than TSS_{dep} for most measuring periods, which would suggest that a small part of the imported sediment was also deposited within the creek system.

For frame 1, the TSS_F, TSS_E, and TSS_{net} values were small compared to the total sediment masses TSS_{dep} deposited in the tidal creek catchment. This suggests again that tidal exchange of suspended sediment did not take place at frame 1 only but along the entire length of the marsh edge. Similar to the negative water balances that were calculated for frame 1, the negative TSS_{net} values need to be

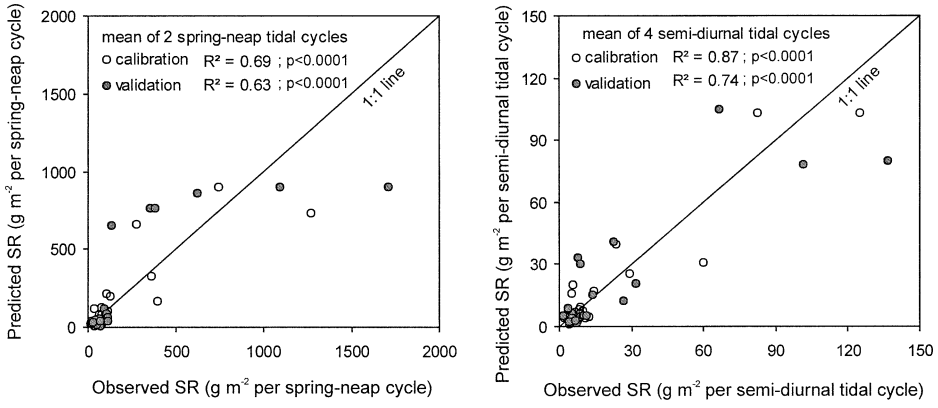

Fig. 7. Observed versus predicted sedimentation rates (SR) using the topography-based model (Eq. 7). Calibration and validation results are presented for the spring-neap data set and the semidiurnal data set.

interpreted as resulting from along-shore sediment transport parallel to the marsh edge rather than from offshore sediment export perpendicular to the marsh edge.

Discussion

Discharge measurements in tidal creeks are widely used to quantify net import or export of water and its constituents (sediments, nutrients, pollutants) to and from tidal marshes (e.g., Reed 1988; Stevenson et al. 1988; Dame et al. 1991; Leonard et al. 1995b; Suk et al. 1999). French and Stoddart (1992) already highlighted that not all material exchange between marshes and the adjacent sea or estuary takes place via tidal creeks; their study demonstrated that about 40% of the total water exchange took place directly via the seaward marsh edge instead of via the creek system. Where the study of French and Stoddart (1992) was limited to only 4 tidal cycles and 1 marsh topography, our present study shows that the percentage of water exchange directly via the marsh edge can vary from about 0% to 60%, and that this variation is related to the high water level for a large number of tidal cycles and the topography for two marsh zones of different developmental stage. This study offers some criticism on the representativeness of traditional field methods used to estimate overall sediment fluxes to tidal marshes: the measurement of tidal creek fluxes and interpolation of spatial sedimentation rate measurements.

Our study shows that for an old, high marsh platform, which is characterized by a deeply-incised creek network with adjoining levees and basins, flow paths are different for tidal inundation cycles with different high water levels: during shallow inundation cycles (high water level $<$ 0.2 m above the creek banks) ca. 100% of all water is supplied to the high marsh platform via the creeks system, while during higher tidal cycles (0.2–0.6 m) the percentage of water directly supplied via the marsh edge increases with increasing high water level (Fig. 8). The presence of this threshold of 0.2 m may be explained as follows. During shallow inundation cycles ($<$ 0.2 m), the tidal wave enters the marsh more easily via the creeks system, while sheet flow coming from the marsh edge over the marsh platform is probably obstructed by the marsh vegetation (about 0.2–0.3 m high) or by small-scale elevation differences between levees and basins (also about 0.2–0.3 m in the study area). During higher tidal cycles (0.2–0.6 m), which overtop the vegetation cover and levees, unobstructed sheet flow becomes possible between the seaward marsh edge and the inner marsh. As a consequence, the percentage of water supplied via the marsh edge increases with increasing high water

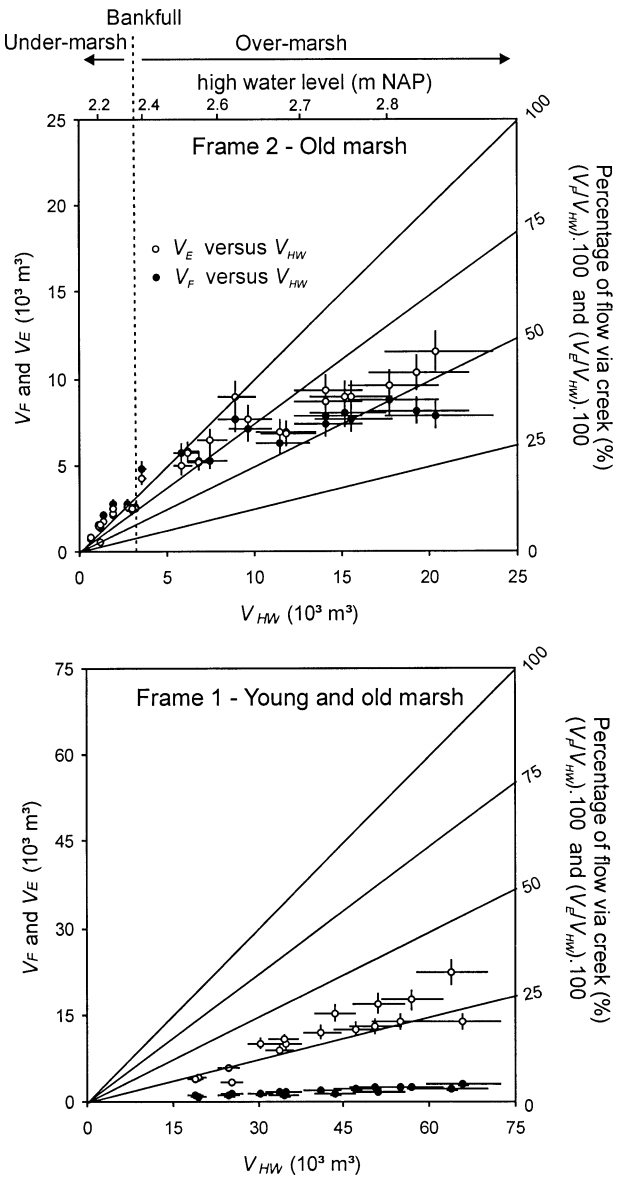

Fig. 8. Water balances for semidiurnal tides with different high water levels: comparison of calculated water volumes discharged through the creeks system during flood (V_F) and ebb (V_E) (Eq. 1) at frame 2 and calculated total water volume stored at high tide (V_{HW}) (Eq. 4) above the old marsh part of the studied creek catchment; comparison of V_F and V_E calculated for frame 1 and V_{HW} calculated for both the young and old marsh. The diagonal lines represent isolines of percentage of total water volume that is supplied via the creek system (i.e., $(V_F/V_{HW}) \times 100$ for the flood and $(V_E/V_{HW}) \times 100$ for the ebb). For the construction of the error bars, see text.

level. Although the percentage of water supplied via the creeks system decreases, the absolute water volume supplied via the creek system still increases with increasing high water level (Fig. 8). This suggests that, even during high tidal cycles, flow via the creeks to the marsh platform still occurs, but

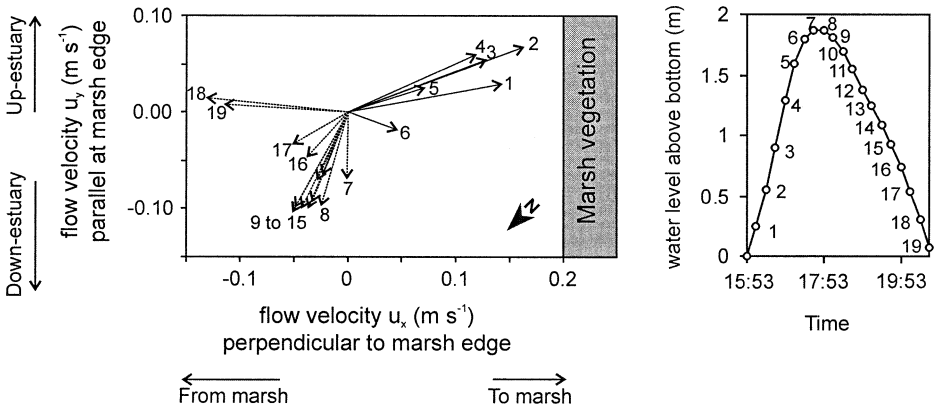

Fig. 9. Example of how flow velocities and directions change during a typical semidiurnal tidal cycle (July 28, 2002) at frame 1 at the seaward marsh edge. For the orientation of the flow velocity components u_x and u_y, see Fig. 1. A north arrow and the marsh vegetation edge are indicated to orientate Fig. 9 relative to Fig. 1. Bold flow vectors represent the flood phase, dashed vectors represent the ebb phase. Numbers at the end of each flow vector indicate subsequent 15-min periods. Corresponding time-water level curve with indication of the 15-min periods by dots.

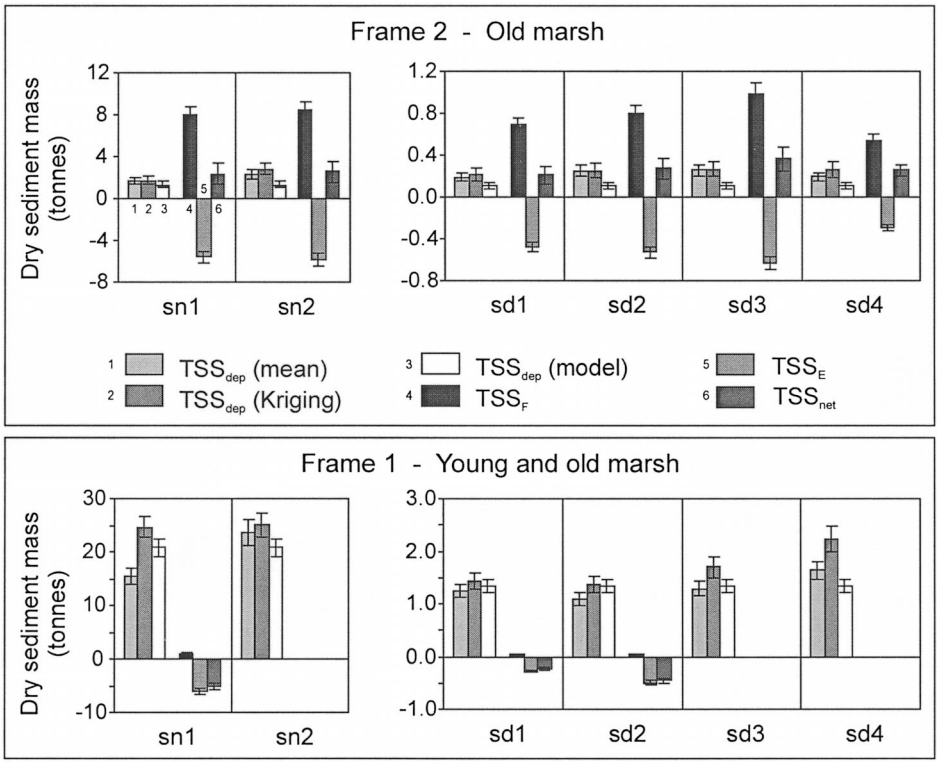

Fig. 10. Sediment balances for two biweekly spring-neap cycles (sn1: August 5–20, 2002; sn2: September 2–16, 2002) and for four semidiurnal tidal cycles (sd1: August 11, 2002; sd2: August 12, 2002; sd3: September 10, 2002; sd4: September 11, 2002): comparison of total suspended sediment mass deposited on the marsh surface (TSS_{dep}), calculated by arithmetic averaging (TSS_{dep} (mean)), by Kriging (TSS_{dep} (Kriging)), and by spatial modeling (TSS_{dep} (model)) of surface sedimentation rate measurements, and total suspended sediment mass transported through the creek system during flood (TSS_F), during ebb (TSS_E) (Eq. 5) and net tidal flux (TSS_{net}) (Eq. 6). No sediment balances are presented for frame 1 for sn2, sd3, sd4 because of gaps in the data records. For the construction of the error bars, see text.

is partly mixed with the larger scale sheet flow coming from the marsh edge.

The latter pattern of mixed flow via the creeks and the marsh edge during high inundation cycles (> 0.2 m) seems to correspond to the few studies in which flow velocities and directions were measured above the marsh platform along a transect perpendicular to tidal creeks. Wang et al. (1993) and Leonard (1997) reported that at the beginning and end of an inundation cycle, flow directions were more or less perpendicular to tidal creeks, while during peak flood and ebb flow directions were more perpendicular to the seaward marsh edge. While these studies were limited to a few tidal cycles (probably only cycles that overtopped the vegetation?), our study includes a wide range of tidal cycles and suggests that flow paths are different between tidal cycles with different high water level; during shallow inundation cycles, we would not expect to see flow perpendicular to the marsh edge but only flow perpendicular to creeks. We lack direct observations on flow directions above the marsh platform to confirm this.

The flooding of marsh platforms starting from creeks is confirmed by the occurrence of flow velocity peaks in creeks, at the moment of flooding and draining of the surrounding marsh platform. This was observed in the study area (Fig. 4) and has been widely reported from other marsh systems (Bayliss-Smith et al. 1979; Dankers et al. 1985; Reed 1989; French and Stoddart 1992). These flow velocity peaks are explained by the sudden increase in the water volume that needs to be transported through the creek at the moment of flooding of the marsh platform starting from the creeks (Pethick 1980; Allen 1994).

Our analysis of sediment fluxes indicated that most sediment, which is deposited on the high marsh platform, is supplied via the creek system. At first sight, this seems to conflict with the water balances, which showed that during high overmarsh tides considerable amounts of water are also transported as sheet flow coming from the marsh edge. The observation that most sediment, which is deposited on the high marsh, is supplied via the creeks system, may be explained by higher SSC in the flooding water in the creeks than above the vegetated marsh surface (e.g., Stumpf 1983; Wang et al. 1993; Leonard et al. 1995a). Before the sheet flow reaches the old marsh, the water passes over the vegetated young marsh, where flow velocities are slowed down and most sediment already settles out from suspension, as reflected by the spatial sedimentation pattern (Fig. 6). On the contrary, the concentrated creek flow forces the water to flow at higher velocities, which are able to transport suspended sediments farther into the marsh.

Our study demonstrates that flow paths are completely different for a young, low marsh, which is typified by a gently seaward sloping topography without a dense creek network and without levee-basin topography. In this case, material transport does not take place predominantly via creeks but across the entire length of the marsh edge. No flow velocity peaks are observed (Fig. 4), since the low marsh is not flooded at once starting from creeks but rather gradually starting from the marsh edge. Flow directions are changing during a tidal cycle from perpendicular to the marsh edge at the beginning and end of inundation to more or less parallel to the marsh edge around maximum inundation (Fig. 9). This is similar to flow patterns relative to tidal marsh creeks on high marsh platforms (see above), but in this case on a much larger scale, relative to the nearby estuarine stream channel (Fig. 1); during maximum inundation the low marsh becomes part of the general water movement in the estuary (e.g., Davidson-Arnott et al. 2002), which is in this case parallel at the axis of the estuarine stream channel.

These differing flow paths on a high, old marsh platform and low, young, seaward sloping marsh have their implications for the spatial sedimentation pattern. We showed that on the high marsh platform, spatial variations in sedimentation rates are related to elevation, distance from the creeks as well as distance from the marsh edge, measured along the creek system (Table 2) (e.g., see also French and Spencer 1993; Leonard 1997; Temmerman et al. 2003; Bartholdy et al. 2004). This agrees very well with the results from the water and sediment balances. During its transport pathway via the creeks and from the creeks over the high marsh platform, suspended sediments progressively settle out, resulting in the observed creek-related sedimentation pattern. On the young marsh spatial variations in sedimentation rates are most related to elevation differences and distance from the marsh edge only (Table 2). Because of its generally seaward sloping topography and the lack of tidal creeks, the young marsh is gradually inundated starting from the marsh edge, so that spatial differences in inundation time, determined by spatial elevation differences, exert most control on the spatial sedimentation pattern.

This study identified some disadvantages of traditional field methods. Overall sediment flux calculations, based on averaging or spatial interpolation of surface sedimentation measurements (e.g., Stoddart et al. 1989; French et al. 1995; Leonard 1997), are very sensitive to the spatial sampling network that is used; e.g., it was shown that an overrepresentation of creek bank sites in the sampling network may lead to overestimation of the overall

sediment budget. In this respect, the presented topography-based modeling approach accounts for the basic mechanisms controlling spatial variations in sedimentation rates and is much less sensitive to the spatial sampling network.

This study also showed that the traditional measurement of tidal creek fluxes, in order to estimate overall material fluxes to tidal marshes (e.g., Ward 1981; Reed 1988; Leonard et al. 1995b; Suk et al. 1999), does not work in all cases. Especially for low, young marshes without a well-developed creek network, it is obvious that flux measurements at the marsh edge are not representative. It is also not straightforward to multiply marsh edge fluxes by the length of the marsh edge, because flow patterns are not unidirectional (perpendicular to the marsh edge) but changing over a tidal cycle in two dimensions. For high, old marsh platforms dissected by a dense tidal creek network, creek flux measurements are only representative for shallow inundation cycles (high water level < 0.2 m above the marsh platform). For higher tides, creek flux measurements result in underestimation of net material budgets because of the increasing importance of material exchange via the marsh edge. The presented approaches of digital elevation modeling and spatial sedimentation modeling allow a reliable estimation of water, sediment, and nutrient budgets.

Acknowledgments

This research was funded by several sources, including the Institute for the Promotion of Innovation by Science and Technology in Flanders (IWT), Delft Cluster, WL|Delft Hydraulics, Rijksinstituut voor Kust en Zee (RIKZ), and Netherlands Institute of Ecology (NIOO), whose support is all gratefully acknowledged. We thank the Rijksinstituut voor Integraal Zoetwaterbeheer en Afvalwaterbehandeling (RIZA) and Directie Oost Nederland (DON) for borrowing equipment free of charge. Finally, we wish to thank Bas Blok, Bas Koutstaal, Jos van Soelen, and Joop van der Pot for their help during the field work. This is NIOO publication number 3495.

Literature Cited

Allen, J. R. L. 1994. A continuity-based sedimentological model for temperate-zone tidal salt marshes. *Journal of the Geological Society* 151:41–49.

Baltsavias, E. P. 1999. Airborne laser scanning: Basic relations and formulas. *ISPRS Journal of Photogrammetry and Remote Sensing* 54:199–214.

Bartholdy, J., C. Christiansen, and H. Kunzendorf. 2004. Long term variations in backbarrier saltmarsh deposition on the Skallingen peninsula, Danish Wadden Sea. *Marine Geology* 203:1–21.

Bayliss-Smith, T. P., R. Healey, R. Lailey, T. Spencer, and D. R. Stoddart. 1979. Tidal flow in salt marsh creeks. *Estuarine Coastal and Shelf Science* 9:235–255.

Boon, J. D. 1978. Suspended solids transport in a salt marsh creek: An analysis of errors, p. 147–159. *In* B. J. Kjerfve (ed.), Estuarine Transport Processes. University of South Carolina Press, Columbia.

Bouma, T. J., M. B. De Vries, E. Low, L. Kusters, P. M. J. Herman, I. C. Tanczos, A. Hesselink, S. Temmerman, P. Meire, and S. Van Regenmortel. 2005. Hydrodynamic measurements on a mudflat and in salt marsh vegetation: Identifying general relationships for habitat characterisations. *Hydrobiologia* 540:259–274.

Claessens, J. and L. Meyvis. 1994. Overzicht van de tijwaarnemingen in het Zeescheldebekken gedurende het decennium 1981–1990. Ministerie van de Vlaamse Gemeenschap AWZ Afdeling Maritieme Schelde, Antwerpen, Belgium.

Dame, R. F., J. D. Spurrier, T. M. Williams, B. Kjerfve, R. G. Zingmark, T. G. Wolaver, T. H. Chrzanowski, H. N. McKellar, and F. J. Vernberg. 1991. Annual material processing by a salt marsh-estuarine basin in South Carolina, USA. *Marine Ecology Progress Series* 72:153–166.

Dankers, N., M. Binsberger, K. Zegers, R. Laane, and M. R. Van de Loeff. 1985. Transport of water, particulate and dissolved organic and inorganic matter between a salt marsh and the Ems-Dollard Estuary, The Netherlands. *Estuarine Coastal and Shelf Science* 19:143–165.

Davidson-Arnott, R. G. D., D. Van Proosdij, J. Ollerhead, and L. Schostak. 2002. Hydrodynamics and sedimentation in salt marshes: Examples from a macrotidal marsh, Bay of Fundy. *Geomorphology* 48:209–231.

Eastman, R. 1994. IDRISI for Windows 2.0 Users Guide. Clark University, Worcester, Massachusetts.

French, J. R. 2003. Airborne LiDAR in support of geomorphological and hydraulic modelling. *Earth Surface Processes and Landforms* 28:321–335.

French, J. R. and T. Spencer. 1993. Dynamics of sedimentation in a tide-dominated backbarrier salt marsh, Norfolk, U.K. *Marine Geology* 110:315–331.

French, J. R., T. Spencer, A. L. Murray, and N. S. Arnold. 1995. Geostatistical analysis of sediment deposition in two small tidal wetlands, Norfolk, U.K. *Journal of Coastal Research* 11:308–321.

French, J. R. and D. R. Stoddart. 1992. Hydrodynamics of salt marsh creek systems: Implications for marsh morphological development and material exchange. *Earth Surface Processes and Landforms* 17:235–252.

Leonard, L. A. 1997. Controls on sediment transport and deposition in an incised mainland marsh basin, southeastern North Carolina. *Wetlands* 17:263–274.

Leonard, L. A., A. C. Hine, and M. E. Luther. 1995a. Surficial sediment transport and deposition processes in a *Juncus-Roemerianus* marsh, west-central Florida. *Journal of Coastal Research* 11:322–336.

Leonard, L. A., A. C. Hine, M. E. Luther, R. P. Stumpf, and E. E. Weight. 1995b. Sediment transport processes in a west-central Florida open marine marsh tidal creek—The role of tides and extra-tropical storms. *Estuarine Coastal and Shelf Science* 41:225–248.

Measures, R. M. 1991. Laser Remote Sensing: Fundamentals and Applications. Krieger Publishing, Melbourne, Australia.

Pethick, J. S. 1980. Velocity surges and asymmetry in tidal channels. *Estuarine Coastal and Shelf Science* 11:331–345.

Reed, D. J. 1987. Temporal sampling and discharge asymmetry in salt marsh creeks. *Estuarine Coastal and Shelf Science* 25:459–466.

Reed, D. J. 1988. Sediment dynamics and deposition in a retreating coastal salt marsh. *Estuarine Coastal and Shelf Science* 26:67–79.

Reed, D. J. 1989. Patterns of sediment deposition in subsiding coastal marshes, Terrebonne Bay, Louisiana: The role of winter storms. *Estuaries* 12:222–227.

Reed, D. J., D. R. Stoddart, and T. P. Bayliss-Smith. 1985. Tidal flows and sediment budgets for a salt-marsh system, Essex, England. *Vegetatio* 62:375–380.

Settlemyre, J. L. and L. R. Gardner. 1977. Suspended sediment

flux through a salt marsh drainage basin. *Estuarine Coastal and Shelf Science* 5:653–663.

STEVENSON, J. C., M. S. KEARNEY, AND E. C. PENDLETON. 1985. Sedimentation and erosion in a Chesapeake Bay brackish marsh system. *Marine Geology* 67:213–235.

STEVENSON, J. C., G. W. LARRY, AND K. S. MICHAEL. 1988. Sediment transport and trapping in marsh systems: Implications of tidal flux studies. *Marine Geology* 80:37–59.

STODDART, D. R., D. J. REED, AND J. R. FRENCH. 1989. Understanding salt marsh accretion, Scolt Head Island, north Norfolk, England. *Estuaries* 12:228–236.

STUMPF, R. P. 1983. The process of sedimentation on the surface of a salt marsh. *Estuarine Coastal and Shelf Science* 17:495–508.

SUK, N. S., Q. GUO, AND N. P. PSUTY. 1999. Suspended solids flux between salt marsh and adjacent bay: A long-term continuous measurement. *Estuarine Coastal and Shelf Science* 49:61–81.

TEMMERMAN, S., G. GOVERS, S. WARTEL, AND P. MEIRE. 2003. Spatial and temporal factors controlling short-term sedimentation in a salt and freshwater tidal marsh, Scheldt estuary, Belgium, SW Netherlands. *Earth Surface Processes and Landforms* 28:739–755.

VAN DAMME, S., B. DE WINDER, T. YSEBAERT, AND P. MEIRE. 2001. Het 'bijzondere' van de Schelde: De abiotiek van het Scheldeestuarium. *De Levende Natuur* 102:37–39.

VAN HEERD, R. M. AND R. J. VAN'T ZAND. 1999. Productspecificatie Actueel Hoogtebestand Nederland. Rijkswaterstaat Meetkundige Dienst, Delft, The Netherlands.

WANG, F. C., T. S. LU, AND W. B. SIKORA. 1993. Intertidal marsh suspended sediment transport processes, Terrebonne Bay, Louisiana, U.S.A. *Journal of Coastal Research* 9:209–220.

WARD, L. G. 1981. Suspended-material transport in marsh tidal channels, Kiawah Island, South Carolina. *Marine Geology* 40: 139–154.

WEBB, K. L., R. WETZEL, T. G. WOLAVER, AND J. C. ZIEMAN. 1983. Tidal exchange of nitrogen and phosphorus between a mesohaline vegetated marsh and the surrounding estuary in the lower Chesapeake Bay. *Estuarine Coastal and Shelf Science* 16: 321–332.

Received, June 4, 2004
Revision, November 30, 2004
Accepted, March 2, 2005